THE JOURNAL OF BIOLOGICAL CHEMISTRY
Vol. 277, No. 45, Issue of November 8, pp. 42633–42638, 2002
Printed in U.S.A.
© 2002 by The American Society for Biochemistry and Molecular Biology, Inc.

Identification and Characterization of Tyrosyl Radical Formation in *Mycobacterium tuberculosis* Catalase-Peroxidase (KatG)*

Received for publication, August 2, 2002, and in revised form, August 27, 2002
Published, JBC Papers in Press, August 29, 2002, DOI 10.1074/jbc.M207916200

Salem Chouchane, Stefania Girotto, Shengwei Yu, and Richard S. Magliozzo‡

From the Department of Chemistry, Brooklyn College and the Graduate Center of the City University of New York, Brooklyn, New York 11210

The catalytic function of *Mycobacterium tuberculosis* catalase-peroxidase (KatG) and its role in activation of the anti-tuberculosis antibiotic isoniazid were investigated using rapid freeze-quench electron paramagnetic resonance (RFQ-EPR) experiments. The reaction of KatG with peroxyacetic acid was followed as a function of time using x-band EPR at 77 K. A doublet EPR signal appears within 6.4 ms after mixing and at time points through hundreds of milliseconds. Thereafter, a singlet signal develops and finally predominates after 1 s, with a total yield of radical ~0.5 spin/heme. Simulation of the spectra provided EPR parameters consistent with those for tyrosyl radicals. Changes in the hyperfine splitting and/or line width in spectra for L-3,3-[$^2H_2$]tyrosine-labeled, but not L-2,4,5,6,7-[$^2H_5$]tryptophan-labeled KatG confirmed this assignment. The initial rate of radical formation was unchanged using a 3-fold or 10-fold excess of peroxyacetic acid, consistent with a rate-determining step involving an intermediate. Although Compound I is likely to be the precursor of tyrosyl radical in KatG, neither its EPR signal nor its reduction to Compound II during formation of the radical(s) could be observed. The tyrosyl radical doublet signal was rapidly quenched by addition of isoniazid and benzoic hydrazide, but not by iproniazid, which binds poorly to KatG.

Catalase-peroxidases are multimeric heme enzymes found in bacteria and other microorganisms. These enzymes, although assigned as Class I peroxidases based on sequence homologies to yeast cytochrome *c* peroxidase and ascorbate peroxidase (1) generally exhibit high catalase activity as well as peroxidase activity with a range of artificial electron donors. In pathogenic mycobacteria, there is a single catalase-peroxidase (KatG)[1] considered important in oxidative stress management and virulence (2, 3), which is also responsible for activation of the antibiotic isoniazid (isonicotinic acid hydrazide, INH). This drug has been successfully used to treat tuberculosis infections since the 1950's (4), although a comprehensive picture of its mechanism of action is only now beginning to emerge. The association between KatG activity and the efficacy of INH, a *pro* drug, was shown through various approaches (5–7). Experimental evidence for formation of radicals in systems containing catalase-peroxidase and INH (8–11) suggested that single electron transfer processes produce drug activation, although a detailed chemical mechanism for formation of the ultimate bactericidal molecule, currently believed to be an acylated nicotinamide adenine dinucleotide cofactor (12, 13), is not yet defined.

Optical stopped-flow experiments have shown that *Mycobacterium tuberculosis* KatG, like other peroxidases, forms the oxyferryl iron porphyrin π-cation radical known as Compound I (Cmpd I) when the resting (ferric) enzyme is treated with alkyl hydroperoxides (14). Catalase-peroxidases from other organisms behave similarly (15, 16). *M. tuberculosis* KatG Cmpd I could be reduced by various substrates including INH, though optical evidence for Compound II was not found in these reactions. In the case of horseradish peroxidase, the expected reduction of Cmpd I to Cmpd II by INH demonstrated that the antibiotic could serve as a single-electron reducing substrate in both steps of a peroxidase cycle (14).

KatG Cmpd I decays relatively rapidly in the absence of exogenous substrates, suggesting that endogenous electron transfers produce amino acid-based radicals during the process. This idea had also been suggested from optical experiments on other catalase-peroxidases (15–18), in which an intermediate labeled Compound II, but exhibiting an optical spectrum closely resembling the resting enzyme, was suggested to contain an unidentified oxidized amino acid that is not electronically coupled to the heme. In an effort to investigate this possibility and further characterize the catalytic pathway in KatG, we have undertaken rapid freeze-quench electron paramagnetic resonance (RFQ-EPR) spectroscopy experiments. In this approach, the resting (ferric) enzyme is mixed with peroxide and allowed to react for various periods of time, followed by rapid freezing of the mixture to quench the reaction; EPR spectroscopy is then used to examine the products. In double mixing experiments, isoniazid or analogues can be added to KatG pre-incubated with peroxyacetic acid. The results presented below demonstrate the formation of tyrosyl radical in high yield from the resting enzyme treated with alkyl peroxide, allowing reassignment of an EPR spectrum previously thought to arise from Cmpd I. We have also attempted to identify the key tyrosine residue(s) involved using site-directed mutagenesis. The observations presented here distinguish the behavior of this enzyme from other Class I peroxidases.

EXPERIMENTAL PROCEDURES

Materials—Escherichia coli UM262 (pKAT II (overexpression system containing the *M. tuberculosis katG* gene) was a gift from Stewart Cole (Institut Pasteur, Paris, France). L-3,3-[$^2H_2$]tyrosine and L-2,4,5,6,7-[$^2H_5$]tryptophan were from Cambridge Isotope Laboratories, Inc. (Cambridge, MA). All other reagents were from Sigma. For some exper-

* This work was supported by National Institutes of Health Grant AI43582 (National Institute of Allergy and Infectious Diseases) and the Heiser Program of the New York Community Trust (to S. Y.). The costs of publication of this article were defrayed in part by the payment of page charges. This article must therefore be hereby marked "*advertisement*" in accordance with 18 U.S.C. Section 1734 solely to indicate this fact.

‡ To whom correspondence should be addressed: Dept. of Chemistry, Brooklyn College, 2900 Bedford Ave., Brooklyn, NY 11210. Tel.: 718-951-4174; Fax: 718-951-4607; E-mail: rmaglioz@brooklyn.cuny.edu.

[1] The abbreviations used are: KatG, catalase-peroxidase; INH, isoniazid (isonicotinic acid hydrazide); Cmpd I, compound I; Cmpd II, compound II; PAA, peroxyacetic acid; PGHS, prostaglandin H synthase; RFQ-EPR, rapid-freeze-quench electron paramagnetic resonance.

This is an Open Access article under the CC BY license.

iments, PAA was treated with catalase to remove hydrogen peroxide prior to use. Isoniazid was recrystallized from methanol.

M. tuberculosis KatG Preparation—M. tuberculosis KatG was prepared from *E. coli* strain UM262 (*katG* minus) carrying an overexpression plasmid (pKAT II) containing the *M. tuberculosis katG* gene according to previously published procedures carried out here in potassium phosphate buffer, pH 7.2 (14, 19). Deuterium-labeled KatG was prepared using the same overexpression plasmid in *E. coli* strain BL21, grown in M9 (minimal) medium containing L-3,3-[$^2H_2$]tyrosine or L-2,4,5,6,7-$^2H_5$]tryptophan (47.6 mg/L) and supplemented with $MgSO_4 \cdot 7\ H_2O$ (0.5 g/L), $CaCl_2 \cdot 2\ H_2O$ (11 mg/L), $ZnCl_2$ (0.5 mg/L), $MnSO_4 \cdot H_2O$ (0.1 mg/L), $FeCl_2 \cdot 4\ H_2O$ (10 mg/L), glucose (3.60 g/L), and δ-aminolevulinic acid-HCl (16.8 mg/L). Although the *E. coli* BL21 strain expresses catalase-peroxidase, no *E. coli* enzyme could be detected by SDS-PAGE of crude extracts from cells grown for 6 h. BL21 strain grew rapidly in minimal medium, which could not be achieved using UM262, which prevented the labeling experiment in this strain. Mutagenesis was performed as described elsewhere (20).

RFQ-EPR Spectroscopy—Rapid freeze-quench EPR samples were prepared as previously described (21) using an Update Instrument, Inc. Model 1000 chemical-freeze-quench apparatus. KatG (typically 100 μM heme) and peroxyacetic acid (3- or 10-fold excess over heme) were mixed and aged for the indicated time periods (all in 20 mM potassium phosphate buffer, pH 7.2) followed by freeze-quenching of reaction mixtures in isopentane at −130 °C. Frozen sample powders were packed into precision-bore quartz EPR tubes immersed in an isopentane bath and were examined using a Varian EPR spectrometer operating at X-band. A finger Dewar inserted into the EPR cavity was used for recording spectra at liquid nitrogen (77 K) temperature, while a liquid helium cryostat and Heli-Tran liquid helium transfer system (Advanced Research Systems, Inc., Allentown, PA) were used for EPR at 5.5 K. EPR data acquisition and manipulation was made using WinEPR software (14). Simulation of EPR spectra was performed using software provided by F. Neese (22, 23). Cu(II)EDTA in 50% ethylene glycol was used as a standard for spin quantification by double integration of EPR signal intensities for radical signals. The signal-to-noise ratio in EPR spectra was improved by signal averaging when necessary. The estimation of spin concentration in freeze-quench samples included application of a packing factor of 0.5 to account for dilution by isopentane. Intensity estimation for the EPR signals of resting enzyme was performed by measurement of the peak height taken at g = 6. This information was used to plot loss of ferric iron signal intensity based on a maximum (100%) signal height for the resting enzyme before reaction with peroxide, again taking into account a packing factor of 0.5.

For double mixing RFQ-EPR experiments, KatG (150 μM) was mixed with peroxyacetic acid (450 μM) and aged for 500 ms in the first reactor hose. This mixture was then mixed with either phosphate buffer or isoniazid, benzoic hydrazide, or iproniazid (isonicotinic acid 2-isopropyl hydrazide) solutions in the same buffer, and aged for an additional 4.2 ms, 200 ms, or 5 s in the second reactor before freeze-quenching and packing as above. The final concentrations after double-mixing were: KatG, 50 μM; PAA, 150 μM; INH or analogue, 7.7 mM. (A high concentration of INH and analogues was used to allow reactions with tyrosyl radical to occur rapidly with respect to the evolution of the doublet signal in the absence of these substrates.) The frozen samples were then examined by EPR as described above.

Optical stopped-flow spectrophotometry was performed using a HiTech Scientific Model SF-61DX2 apparatus equipped with a rapid-scanning diode-array spectrophotometer and Kinet-Asyst software for data acquisition and analysis. The concentrations of KatG (50 μM final) and PAA (150 μM) were the same as those used for the single mixing RFQ-EPR experiments. Formation of Cmpd I was confirmed and the $t_{1/2}$ was evaluated from the increase in absorbance at 590 nm, rather than the loss of absorbance in the Soret region, as previously described (14).

RESULTS

Rapid freeze-quench EPR spectroscopy experiments combined with characterization of the observed EPR spectra and isotopic substitution experiments demonstrated the formation of tyrosyl radicals in *M. tuberculosis* KatG in reactions with peroxyacetic acid (or *m*-chloroperoxybenzoic acid). The kinetics and stoichiometry of radical formation, and an analysis of the proton hyperfine couplings based on simulation of the EPR signals, and quenching of the radical by INH, is also presented.

Identification of Tyrosyl Radical—Fig. 1 shows the progress of the reaction of ferric (resting) *M. tuberculosis* KatG with peroxyacetic acid from 50 ms to 10 s after mixing in a typical RFQ-EPR experiment (g = 2 region). A doublet signal was detected within 6.4 ms of mixing (data not shown), which is the earliest time point experimentally accessible. The initial doublet signal, observable through ~500 ms (Fig. 1, *a–d*) is characterized by a principal hyperfine splitting of ~ 19 gauss and a linewidth of ~30 gauss (peak to trough). The singlet signal centered at g = 2.004, seen in the same reaction mixture after a longer time of incubation (Fig. 1*g*) has a line width of 27 gauss and weak hyperfine features. The same signals were obtained when *m*-chloroperoxybenzoic acid was used in place of peroxyacetic acid (data not shown). Examination of these samples at 5.5 K allowed observation of the decrease in ferric iron signal intensity in the g = 6 region during this time course (see below).

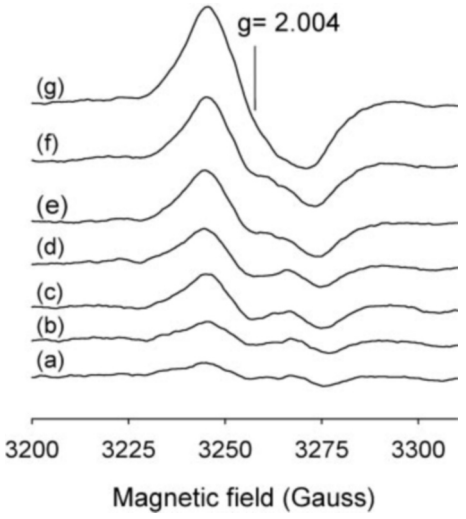

FIG. 1. **Evolution of tyrosyl radical EPR spectra as a function of time.** KatG (50 μM final) was reacted at 25 °C with PAA (150 μM final) in 20 mM potassium phosphate buffer (pH = 7.2). Reaction mixtures were freeze-quenched after 50 ms (*a*), 100 ms (*b*), 250 ms (*c*), 500 ms (*d*), 2 s (*e*), 5 s (*f*), and 10 s (*g*). The EPR spectra were recorded at 77 K (microwave frequency 9.13 GHz, modulation amplitude 4 G, microwave power 5 mW).

Simulation of the doublet and singlet spectra (Fig. 2) was achieved using the parameters given in Table I. The g-tensor values and proton hyperfine couplings were taken to be similar to those reported elsewhere for tyrosyl radicals (24, 25), whereas the β-methylene hydrogen nuclear hyperfine coupling parameters were varied to achieve the simulation. Although the doublet EPR signal may contain some small fraction of signal intensity due to the singlet, no correction for overlap was made, because the spectrum shown could be adequately simulated using a single set of parameters, as was the singlet recorded after 10 s. Although assignment of both signals to tyrosyl radicals could be made based on simulation parameters, a similar doublet signal may also arise from a neutral tryptophanyl radical (26). This is due to the fact that the principal hyperfine splitting in the doublet signals arises from the coupling of unpaired electron spin in the π systems of phenol or indole rings with one of the β-methylene hydrogens of both tyrosyl and tryptophanyl radicals (24, 26). For this reason, RFQ-EPR experiments were performed using isotopically labeled KatG.

Deuterium-labeled KatG was prepared by enzyme overexpression in bacteria grown in minimal medium containing tryptophan labeled in the indole ring (2,4,5,6,7-[$^2H_5$]tryptophan) or tyrosine labeled at the β-methylene group (3,3-[$^2H_2$]tyrosine). Uptake of these amino acids and their incorporation into polypeptides in the bacteria expressing KatG affords specific

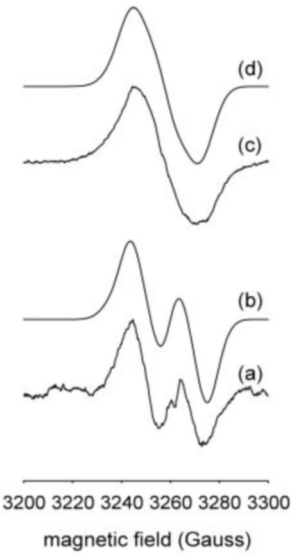

FIG. 2. **Simulation of tyrosyl radical doublet and singlet EPR spectra.** Spectra *a* and *c* are the experimental spectra taken from Fig. 1, *c* and *g* (250 ms and 10 s, respectively); spectra *b* and *d* are simulations based on the parameters given in Table I.

TABLE I
EPR parameters evaluated by simulation of tyrosyl radical doublet and singlet signals

The g-tensor values are not resolved at X-band, nor are the weak (ring hydrogen) hyperfine couplings. The weak hyperfine couplings do not vary greatly for the tyrosyl radicals found in various systems, although the g_x value can vary depending on the hydrogen-bonding environment of the phenolic oxygen (35,46). Here, the g-tensor values and the 3,5-ring proton coupling values are essentially the same as those reported in (24).

	$g_{(x,y,z)}$	$A_{(xx,yy,zz)}$ MHz (β-methylene proton)	$A_{(xx,yy,zz)}$ MHz (3,5-ring protons)
Doublet signal	2.0087	47.5	23.7
	2.0044	47.5	7.4
	2.0023	50.0	19.5
Singlet signal	2.0074	34.0	26.0
	2.0044	34.0	7.8
	2.0023	37.0	20.9

labeling of the enzyme with the desired isotope. This approach was based on methodology used to identify tyrosyl radical in ribonucleotide reductase (27, 28) and in prostaglandin H synthase (29). Rapid-freeze-quench EPR samples were then prepared as above, using the purified, labeled enzymes. Fig. 3 shows a comparison of the doublet and singlet signals formed in unlabeled KatG with spectra recorded using the [^{2}H]tryptophan- and [^{2}H]tyrosine-labeled enzymes. No change in the initial doublet signal occurred for KatG containing deuterium-labeled tryptophan (Fig. 3*d*; compare with the unlabeled tryptophan shown in Fig. 3*c*). For KatG containing deuterium-labeled tyrosine, an initial singlet (17 gauss line width) (Fig. 3*e*) was found in place of the doublet. The line width of the singlet seen at 10 s in [^{2}H]tyrosine-labeled KatG (Fig. 3*b*) was reduced (15 gauss *versus* 27 gauss) compared with the signal in unlabeled enzyme at this time point (Fig. 3*a*). These changes reflect a reduction in nuclear hyperfine coupling accompanying incorporation only of deuterium-labeled tyrosine into the enzyme and thereby confirm the identity of both signals as tyrosyl radicals. The change from doublet to singlet and the more subtle change in the spectrum of the singlet signal are both consistent with a reduction of the strong hyperfine coupling to one of the β-methylene hydrogens in the radicals. These changes could be reproduced in simulations (not shown) of the EPR spectra by scaling the hydrogen nuclear hyperfine coupling parameters given above by the factor ($g_n(^2H)/g_n(^1H)$ = 0.1535) to account for the weaker coupling in deuterium-labeled enzyme.

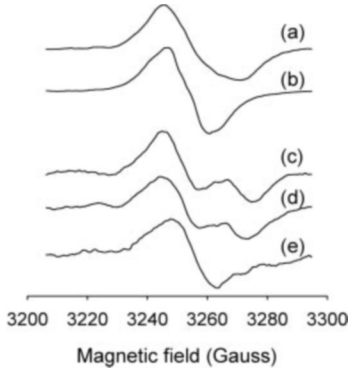

FIG. 3. **EPR spectra of radical species formed in deuterium-labeled KatG.** Labeled or unlabeled KatG (50 μM final) was reacted at 25 °C with PAA (150 μM final) in 20 mM potassium phosphate buffer (pH = 7.2). *a*, unlabeled KatG, 10 s reaction; *b*, L-3,3-[$^2H_2$]tyrosine-labeled KatG, 10 s reaction; *c*, unlabeled KatG, 250 ms reaction; *d*, L-2,4,5,6,7-[$^2H_5$]tryptophan-labeled KatG, 200 ms reaction; *e*, L-3,3-[$^2H_2$]tyrosine-labeled KatG, 250 ms reaction. EPR spectra were recorded under the same conditions as described in Fig. 1.

Kinetic Analysis—Quantitative RFQ-EPR was performed to evaluate the total yield of radical with respect to heme concentration, using both a 3-fold and a 10-fold excess of peroxide over heme. The plot shown in Fig. 4*A* presents the concentration of the radical expressed as spin/heme, as a function of time. The slower generation of the singlet follows the initial phase due to formation of the doublet species. The maximum yield of radical was about 0.5 spins per mole of heme at 10 s; beyond 10 s the signal intensity began to decay. The progress of this reaction was the same whether 3-fold or 10-fold excess peroxide was used (data not shown). The initial rate of radical formation, determined by a linear least squares fit of the EPR data for the early time points (0–0.5 s), was 0.18 and 0.19 spin·heme^{-1}·s^{-1} for KatG/peroxide ratios equal to 1:3 and 1:10, respectively. The curve generated from a similar experiment in which hydrogen peroxide-free PAA was used was the same except for a greater yield of radical after 10 s.

The unchanged rate of appearance of radical with increasing peroxide concentration provides evidence for radical formation from an intermediate assumed to be Cmpd I (see below). Examination of RFQ-EPR samples at 5.5 K in the g = 6 region showed a decrease in intensity due to loss of ferric heme iron occurring from the earliest time point accessible (~ 6.4 ms) through 1 s, after which the intensity began to increase (Fig. 4*B*). No signal other than that due to tyrosyl radical or resting enzyme was detected at 5.5 K. These EPR results indicate that the loss of ferric iron under these conditions is faster ($t_{1/2}$ < 50 ms) than the rate of appearance of tyrosyl radical but similar to the rate of formation of Cmpd I estimated from optical stopped-flow measurements under the same conditions ($t_{1/2}$ = 50 ms) (see below). Because an EPR signal characteristic of Cmpd I was not detectable at any time point, no direct kinetic correlation could be drawn between the formation of the radical and the disappearance of a precursor (except Fe^{III}) in this approach.

Optical stopped-flow measurements for reactions of KatG with PAA under the same conditions as the RFQ-EPR experiments were also made. Here, the progress from ferric iron to KatG Cmpd I was complete in ~100 ms using a 3-fold excess of peroxide (Fig. 5). The rate of this reaction increases linearly with peroxide concentration (14). After the formation of Cmpd I, a steady-state absorbance was achieved. The absorbance then slowly returned to its initial value. During this return, no evidence for other intermediates, such as Cmpd II was de-

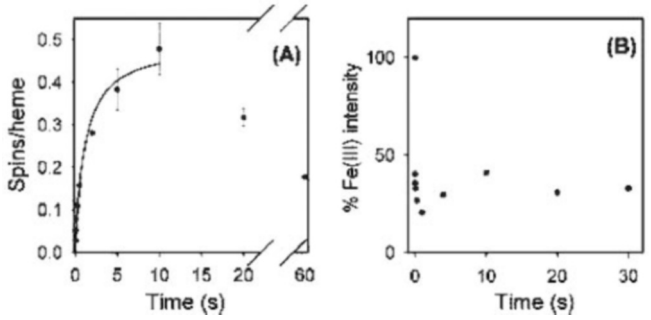

FIG. 4. **Yield (spins/heme) of tyrosyl radical as a function of time.** *A*, concentration of tyrosyl radical was evaluated by double integration of EPR signal intensity (in triplicate RFQ-EPR experiments) using KatG (50 μM final) reacted with PAA (150 μM final) for the time periods given by the data points. *B*, relative intensity due to residual ferric iron evaluated as the signal height at g = 6.0 in spectra recorded at 5.5 K for the same or similar samples used for observation of the g = 2 region.

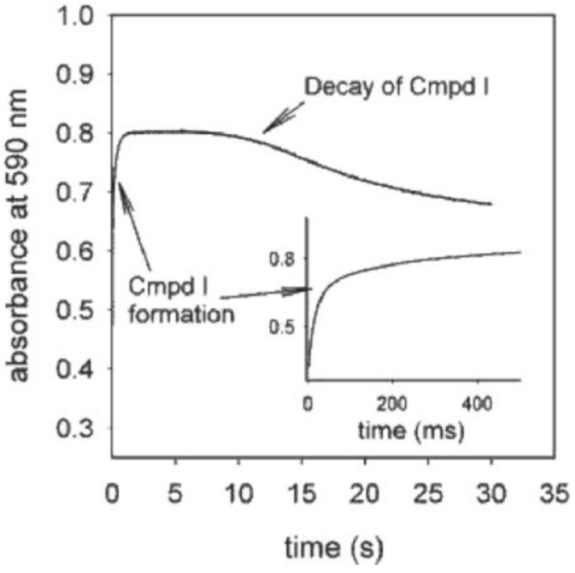

FIG. 5. **Optical stopped-flow data showing formation of KatG Compound I.** Time trace (at 590 nm) recorded for the reaction of KatG (50 μM final) with PAA (150 μM final) in 20 mM potassium phosphate buffer, pH 7.2 at 25 °C. *Inset*, expanded trace, 0–500 ms.

tected. These observations are consistent with the presence of Cmpd I during generation of tyrosyl radical.

Tyrosyl Radical Quenching by INH—Because tyrosyl radical appears during the interval in which Cmpd I formation is reaching a maximum under the conditions chosen here, the kinetic competence of both redox active centers should be taken into account. The reaction of KatG Cmpd I with substrates has been previously demonstrated (14). In order to investigate whether the tyrosyl radical is kinetically competent in reactions with a substrate such as the antibiotic INH and analogues, we have undertaken double-mixing RFQ-EPR experiments. The samples were prepared to allow direct comparison of EPR signal intensities, since both the total reaction time and the final enzyme concentration were normalized using buffer or INH solution in the second mixing step, as follows. KatG was reacted with PAA for 500 ms in the first reactor; this mixture was then mixed with buffer or substrates and incubated for a further 4.2 ms or 200 ms before freeze-quenching. The substrate INH, benzoic hydrazide, or iproniazid was added in the second mixing steps. With INH addition, tyrosyl-radical signal intensity was reduced by 30% after a 4.2-ms reaction (Fig. 6*c*), compared with the sample mixed with buffer alone (Fig. 6*a*).

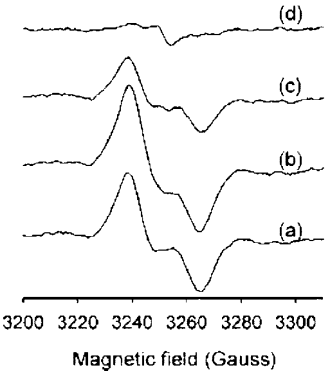

FIG. 6. **Double-mixing rapid freeze-quench EPR of KatG reacted with peroxide and isoniazid.** KatG was reacted with PAA for 500 ms in the first reactor, then with phosphate buffer for 4.2 ms (*a*) or 200 ms (*b*) or with INH for 4.2 ms (*c*) or 200 ms (*d*) followed by freeze-quenching. The EPR spectra were recorded under the same conditions as described in Fig. 1.

After 200 ms in the presence of INH, the EPR signal of the tyrosyl radical was nearly completely quenched (Fig. 6*d*), whereas in its absence (Fig. 6*b*), the intensity doubled from that shown in Fig. 6*a*. Similar results were found using benzoic hydrazide, a drug analogue lacking the pyridine nitrogen (data not shown). With iproniazid, which contains an isopropyl substituent on N(2) of the hydrazide moiety, the extent of quenching was much lower (data not shown). These three hydrazides were chosen because other experiments have shown that INH and benzoic hydrazide bind with high affinity to KatG, whereas no evidence for binding of iproniazid could be demonstrated in a similar concentration range.

The fact that INH was shown previously to react with Cmpd I of KatG (14) would allow that Cmpd I was also reduced by substrates in the double mixing experiments. Removal of Cmpd I may limit the yield of radical if rates of formation of radical and rate of reaction of Cmpd I with substrates were competitive, but Cmpd I reduction would not cause quenching of the tyrosyl radical already formed at any particular time point during the reactions. Therefore, the results show that the addition of substrates caused a rapid loss of tyrosyl radical rather than simply preventing the increase in radical concentration that occurs during the additional incubation period after the second mixing steps (4.2 ms or 200 ms).

Mutagenesis of *M. tuberculosis* KatG, in which several of its 20 tyrosines were separately changed to phenylalanine residues (Tyr-98, Tyr-113, Tyr-155, Tyr-229, Tyr-304, and Tyr-426; many of these tyrosine residues are conserved in KatG enzymes from various sources), failed to produce a mutant in which tyrosyl radical doublet and singlet signals were absent from RFQ-EPR samples. However, in some of these mutants, the kinetics and the mechanism of tyrosyl-radical evolution appear to be different compared with the wild-type enzyme. Further study is ongoing to determine whether these observations indicate that secondary tyrosine residues are oxidized in the mutants, as might be expected given that such results occur in other radical-forming enzymes (30–37).

DISCUSSION

The results described above confirm the formation of tyrosyl radical(s) in high yield in *M. tuberculosis* KatG during reaction of the resting enzyme with alkyl peroxides, differentiating this Class I peroxidase from others. The kinetics of radical formation suggest production of a unique radical center via an intermediate most likely to be Compound I. The observation of the evolution of a doublet EPR signal to a singlet signal provides evidence for structural similarity between the radical in KatG

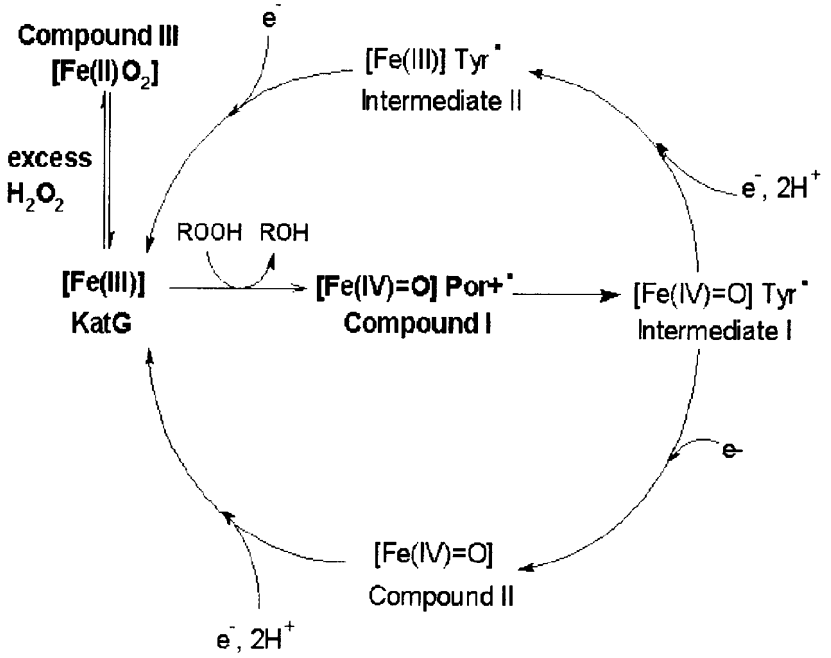

FIG. 7. **Scheme for KatG catalytic cycles.** The species shown in bold text are those identified here or in previous work on KatG (14). Tyr●, tyrosyl radical; Por+●, porphyrin π-cation radical; ROOH, *m*-chloroperoxybenzoic acid, peroxyacetic acid, or *t*-butylhydroperoxide. (This scheme is similar to the one reported for PGHS (25)).

and that in PGHS-1 (24). The catalytic competence of the radical giving rise to the initial doublet EPR signal was demonstrated in reactions with INH and other hydrazides.

Tyrosyl radicals are found in other heme enzymes including mammalian catalase (32), turnip peroxidase isoenzyme 7 (30), and prostaglandin H synthase (25), although a catalytic function has only been defined for PGHS, in which a tyrosyl radical is responsible for cyclooxygenase activity. In this enzyme, a single tyrosyl radical gives rise to both a doublet and singlet EPR signal (24). This behavior has been characterized to be the result of a change in orientation of the phenolic ring with respect to the β-methylene hydrogens of tyrosine. This orientation governs the strength of the interaction of the unpaired electron localized in the π-system of the ring with these hydrogens (24, 38). This interesting behavior may arise from a change in polarity, because the phenolic radical has more anionic character than the protonated phenol ring of tyrosine and may also be driven by thermodynamic factors that are orientation-dependent (24). To date, only singlet EPR signals have been reported for the other enzymes (30, 32). Although the analogies between the behavior observed in the rapid freeze-quench EPR experiments on KatG and the well characterized behavior in PGHS are strong, the possibility remains that the doublet and singlet species seen here represent two different tyrosine residues. This issue is being addressed through site-directed mutagenesis and spin labeling. Sequence alignment of *M. tuberculosis* KatG (39) with PGHS (40, 41) did not indicate a homologous candidate among the 20 tyrosines of KatG for the site of the radical, which occurs on residue Tyr-385 in PGHS-1 (29).

The yield of tyrosyl radical in KatG as a function of time was constant on tripling the ratio of peroxide to heme iron. The constancy in this rate argues against the possibility that heme redox recycling, known to occur in KatG in the presence of excess peroxide (14), produces additional radicals beyond a single turnover. Furthermore, formation of a unique tyrosyl radical is suggested, because no increase in yield occurred under conditions enabling a greater rate of recycling (10-fold excess peroxide) that could have generated more radical after the initial turnover from ferric enzyme to Cmpd I and then tyrosyl radical. Thus, radical generation and heme recycling are uncoupled.

In earlier work on *M. tuberculosis* KatG (14), a singlet EPR signal found when resting enzyme was reacted with *m*-chloroperoxybenzoic acid had been assigned to the porphyrin π-cation radical of Cmpd I.[2] A more comprehensive examination of the characteristics of the singlet EPR spectrum reported earlier was undertaken upon observation of the doublet signal revealed by the rapid freeze-quench EPR approach described here. A singlet EPR signal generated in *E. coli* hydroperoxidase I, another catalase-peroxidase, was also reported to represent the porphyrin π-cation radical of Cmpd I (42). *E. coli* hydroperoxidase I has significant homology to *M. tuberculosis* KatG, including many conserved tyrosines (43), suggesting that the singlet EPR signal seen in that enzyme treated with peroxide may also arise from a tyrosyl radical. We have not found conditions under which a signal around g = 2.0 different from tyrosyl radical could be detected at 5.5 K in samples known from optical stopped-flow measurements to contain Cmpd I. Strong anti-ferromagnetic coupling between the porphyrin π-cation radical and oxyferryl iron (S = 1) could contribute to this phenomenon.

Although activation (or at least oxidation) of INH by KatG has been initiated *in vitro* through various paths starting from resting KatG (44, 45), only KatG Cmpd I (14) and the tyrosyl radical have been directly shown to be kinetically competent in reactions with this antibiotic. The results with small molecules presented here suggest that oxidations or, more likely, hydrogen atom abstractions may be initiated by the tyrosyl radical in a reaction separate from the heme-dependent peroxidase cycle in KatG. Whether the tyrosyl radical in KatG plays a fundamental role in drug activation or whether it may be responsible for some metabolic reaction *in vivo* remains to be demonstrated.

The intermediates potentially formed upon reaction of KatG with peroxides are presented in Fig. 7, although at present we

[2] The spectrometer conditions under which this signal was investigated previously were chosen to facilitate identification of the π-cation radical signal (5.5 K, high microwave power) and at the same time, made observation of the weak hyperfine features in the tyrosyl radical singlet spectrum unfavorable due to saturation. A π-cation radical signal was expected and easily explained because the reaction with peroxide was shown in optical experiments to generate Cmpd I, and the EPR sample exhibited a green color characteristic of Cmpd I.

have spectroscopic information that only accounts for some of them. The reaction pathway to tyrosyl radical in KatG presumably requires formation of Cmpd I, followed by its conversion to Intermediate I through a one-electron transfer step. The complete analysis of the kinetics of radical formation awaits further study, since heme redox changes have not yet been correlated with radical formation.

The tyrosine mutants of KatG tested to date showed formation of tyrosine radical doublet and singlet EPR signals in RFQ-EPR experiments. Additional mutagenesis and other approaches, including covalent labeling of the initially formed radical, are being pursued to help sort out identification of the tyrosine residue(s) in question in KatG.

Acknowledgments—We thank Drs. WenHai Zhang and John Kozarich for their support.

REFERENCES

1. Welinder, K. G., Mauro, J. M., and Norskov-Lauritsen, L. (1992) *Biochem. Soc. Trans.* **20,** 337–340
2. Collins, D. M. (1996) *Trends Microbiol.* **4,** 426–430
3. Pym, A. S., Domenech, P., Honore, N., Song, J., Deretic, V., and Cole, S. T. (2001) *Mol. Microbiol.* **40,** 879–889
4. Robitzek, E. H., and Selikoff, I. J. (1952) *Am. Rev. Tuberc.* **65,** 402–410
5. Zhang, Y., Heym, B., Allen, B., Young, D., and Cole, S. (1992) *Nature* **358,** 591–593
6. Johnsson, K., and Schultz, P. G. (1994) *J. Am. Chem. Soc.* **116,** 7425–7426
7. Johnsson, K., King, D. S., and Schultz, P. G. (1995) *J. Am. Chem. Soc.* **117,** 5009–5010
8. Sinha, B. K. (1983) *J. Biol. Chem.* **258,** 796–801
9. Saint-Joanis, B., Souchon, H., Wilming, M., Johnsson, K., Alzari, P. M., and Cole, S. T. (1999) *Biochem. J.* **338,** 753–760
10. Hillar, A., and Loewen, P. C. (1995) *Arch. Biochem. Biophys.* **323,** 438–446
11. Wengenack, N. L., and Rusnak, F. (2001) *Biochemistry* **40,** 8990–8996
12. Lei, B., Wei, C. J., and Tu, S. C. (2000) *J. Biol. Chem.* **275,** 2520–2526
13. Rozwarski, D. A., Grant, G. A., Barton, D. H. R., Jacobs, W. R., Jr., and Sacchettini, J. C. (1998) *Science* **279,** 98–102
14. Chouchane, S., Lippai, I., and Magliozzo, R. S. (2000) *Biochemistry* **39,** 9975–9983
15. Regelsberger, G., Jakopitsch, C., Engleder, M., Ruker, F., Peschek, G. A., and Obinger, C. (1999) *Biochemistry* **38,** 10480–10488
16. Engleder, M., Regelsberger, G., Jakopitsch, C., Furtmuller, P. G., Ruker, F., Peschek, G. A., and Obinger, C. (2000) *Biochimie (Paris)* **82,** 211–219
17. Obinger, C., Regelsberger, G., Furtmuller, P. G., Jakopitsch, C., Ruker, F., Pircher, A., and Peschek, G. A. (1999) *Free. Rad. Res.* **31,** (suppl), S243–S249
18. Regelsberger, G., Jakopitsch, C., Ruker, F., Krois, D., Peschek, G. A., and Obinger, C. (2000) *J. Biol. Chem.* **275,** 22854–22861
19. Marcinkeviciene, J. A., Magliozzo, R. S., and Blanchard, J. S. (1995) *J. Biol. Chem.* **270,** 22290–22295
20. Yu, S., Chouchane, S., and Magliozzo, R. S. (2002) *Protein Sci.* **11,** 58–64
21. Zhang, W., Wong, K. K., Magliozzo, R. S., and Kozarich, J. W. (2001) *Biochemistry* **40,** 4123–30
22. Neese, F. (1997) *Dissertation*, University of Konstanz, Konstanz, Germany
23. Neese, F. (1995) *Quantum Chemistry Program Exchange Bull.*, p. 5, University of Indiana, Bloomington, IN
24. Shi, W., Hoganson, C. W., Espe, M., Bender, C. J., Babcock, G. T., Palmer, G., Kulmacz, R. J., and Tsai, A. (2000) *Biochemistry* **39,** 4112–4121
25. Tsai, A., Wu, G., Palmer, G., Bambai, B., Koehn, J. A., Marshall, P. J., and Kulmacz, R. J. (1999) *J. Biol. Chem.* **274,** 21695–21700
26. Lendzian, F., Sahlin, M., MacMillan, F., Bittl, B., Fiege, R., Potsch, P., Sjoberg, B.-M., Graslund, A., Lubitz, F., and Lassmann, G. (1996) *J. Am. Chem. Soc.* **118,** 8111–8120
27. Sjoberg, B. M., and Reichard, P. (1977) *J. Biol. Chem.* **252,** 536–541
28. Sjoberg, B. M., Reichard, P., Graslund, A., and Ehrenberg, A. (1978) *J. Biol. Chem.* **253,** 6863–6865
29. Tsai, A., Hsi, L. C., Kulmacz, R. J., Palmer, G., and Smith, W. L. (1994) *J. Biol. Chem.* **269,** 5085–5091
30. Ivancich, A., Mazza, G., and Desbois, A. (2001) *Biochemistry* **40,** 6860–6866
31. Ivancich, A., Dorlet, P., Goodin, D. B., and Un, S. (2001) *J. Am. Chem. Soc.* **123,** 5050–5058
32. Ivancich, A., Jouve, H. M., Sartor, B., and Gaillard, J. (1997) *Biochemistry* **36,** 9356–9364
33. Kulmacz, R. J., Ren, Y., Tsai, A. L., and Palmer, G. (1990) *Biochemistry* **29,** 8760–8771
34. Lu, G., Tsai, A. L., Van Wart, H. E., and Kulmacz, R. J. (1999) *J. Biol. Chem.* **274,** 16162–16167
35. Gerfen, G. J., Bellow, F. B., Un, S., Bollinger Jr., J. M., Stubbe, J., Griffin, G. R., and Singel, J. D. (1993) *J. Am. Chem. Soc.* **115,** 6420–6421
36. Sjoberg, B. M., and Graslund, A. (1977) *CIBA Found. Symp.* **60,** 187–196
37. Sahlin, M., Graslund, A., Ehrenberg, A., and Sjoberg, B. M. (1982) *J. Biol. Chem.* **257,** 366–369
38. Bender, C. J., Sahlin, M., Babcock, G. T., Barry, B. A., Chandrashekar, T. K., Salowe, S. P., Stubbe, J., Lindstroem, B., Petersson, L., Ehrenberg, A., and Sjoberg, B.-M. (1989) *J. Am. Chem. Soc.* **111,** 8076–8083
39. Heym, B., Zhang, Y., Poulet, S., Young, D., and Cole, S. T. (1993) *J. Bacteriol.* **175,** 4255–4259
40. Funk, C. D., Funk, L. B., Kennedy, M. E., Pong, A. S., and Fitzgerald, G. A. (1991) *FASEB J.* **5,** 2304–2312
41. Kosaka, T., Miyata, A., Ihara, H., Hara, S., Sugimoto, T., Takeda, O., Takahashi, E., and Tanabe, T. (1994) *Eur. J. Biochem.* **221,** 889–897
42. Hillar, A., Peters, B., Pauls, R., Loboda, A., Zhang, H., Mauk, A. G., and Loewen, P. C. (2000) *Biochemistry* **39,** 5868–5875
43. Zamocky, M., Regelsberger, G., Jakopitsch, C., and Obinger, C. (2001) *FEBS Lett.* **492,** 177–182
44. Magliozzo, R. S., and Marcinkeviciene, J. A. (1996) *J. Am. Chem. Soc.* **118,** 11303–11304
45. Wengenack, N. L., Hoard, H. M., and Rusnak, F. (1999) *J. Am. Chem. Soc.* **121,** 9748–9749
46. Ivancich, A., Mattioli, T. A., and Un, S. (1999) *J. Am. Chem. Soc.* **121,** 5743–5753